Tuning the Fluorescence Emission Spectra of a Single Molecule with a Variable Optical Subwavelength Metal Microcavity

Alexey Chizhik, Frank Schleifenbaum, Raphael Gutbrod, Anna Chizhik, Dmitry Khoptyar,* and Alfred J. Meixner†
Institute of Physical and Theoretical Chemistry, Eberhard Karls University, 72076 Tübingen, Germany

Jörg Enderlein‡
III. Institute of Physics, Georg August University, 37077 Göttingen, Germany
(Received 21 October 2008; published 18 February 2009)

We present experimental and theoretical results on changing the fluorescence emission spectrum of a single molecule by embedding it within a tunable planar microcavity with subwavelength spacing. The cavity length is changed with nanometer precision by using a piezoelectric actuator. By varying its length, the local mode structure of the electromagnetic field is changed together with the radiative coupling of the emitting molecule to the field. Because mode structure and coupling are both frequency dependent, this leads to a renormalization of the emission spectrum of the molecule. We develop a theoretical model for these spectral changes and find excellent agreement between theoretical prediction and experimental results.

DOI: 10.1103/PhysRevLett.102.073002 PACS numbers: 37.30.+i, 32.50.+d, 33.50.Dq, 42.50.Pq

As was first noted by Purcell more then 60 years ago [1], placing an emitter within a confined geometry alters its emission properties, in particular, the rate of spontaneous emission is increased. This can be easily understood within a Fermi's golden rule approach to the emission of an electric dipole within the given geometry: The density of modes of the electromagnetic field inside a cavity is changed with respect to free space, and hence the coupling of the dipole transition of an emitting molecule to this field. The first extensive experimental studies of the changes in spontaneous emission rates of molecules in front of a metal mirror were conducted by Kuhn and Drexhage (see Ref. [2]), and a comprehensive semiclassical model for these experiments was developed by Chance, Prock and Silbey [3]. Lukosz and coworkers conducted extensive studies of the changes in the angular distribution of radiation of fluorescent molecules close to a metallic mirror or dielectric interfaces [4,5]. Later, all of these results had been confirmed also on a single molecule level, see Ref. [6] and citations therein. Remarkably, little attention has been paid to the changes in the *emission spectrum* of a fluorescent dye as induced by the changes of the local electromagnetic field structure. This is partially due to the fact that when observing molecules with narrow emission bands, optical dispersion of the molecule's environment is rather weak, so that the *wavelength dependence* of the changes in the radiative transition rate by its environment is negligible. However, if a molecule displays a broad emission spectrum, one can no longer neglect optical dispersion effects, and strong shape changes of a molecule's emission spectrum are expected. This is due to the fact that the optical dispersion of a molecule's environment leads to a wavelength-dependent electromagnetic coupling of the emitter to its environment, which results in a renormalization of the observable emission spectrum of the embedded molecule. For example, strong changes in the emission and absorption spectra have been predicted for a Rhodamine6G molecule embedded within a spherical metal nanocavity [7].

Experimentally, this effect has been observed qualitatively by Steiner *et al.* [8] who investigated single isolated perylene dye molecules in a planar metal microcavity for different mirror spacings and hence for different electromagnetic mode structures. However, as the mirror spacing was fixed, they could investigate a distinct molecule only for one given resonator length. In the present Letter, we report on changing the emission spectrum of a single fluorescent molecule embedded in a tunable microcavity. Thus, for the first time we were able to actively change the local electromagnetic field structure around a molecule by changing the mirror spacing of the cavity. In doing that, one selects the vibronic transition where fluorescence will mostly occur. Moreover, we develop a semiclassical theoretical model for these spectral changes, and find excellent agreement between theory and experiment. Together with the well-studied changes of radiative transition rates (fluorescence or luminescence lifetime) and angular distributions of radiation, this is another important step in our understanding of the complex electromagnetic interaction of single photon emitters with an electromagnetic field structure that is tailored by the emitter's surrounding.

The experimental setup is depicted in Fig. 1(a) and is similar to a previously built microcavity but with no adjustable cavity length [8]. A homemade aluminum cavity holder was used to hold the multilayer cavity. The bottom part of the cavity consisted of a coverslip (thickness 170 μm), covered by a thin silver film (47 nm), a silicon oxide layer (30 nm, refractive index $n = 1.46$), a polymer layer (70 nm, refractive index $n = 1.49$) with dissolved dye molecules, and a second thin silicon oxide layer (8 nm,

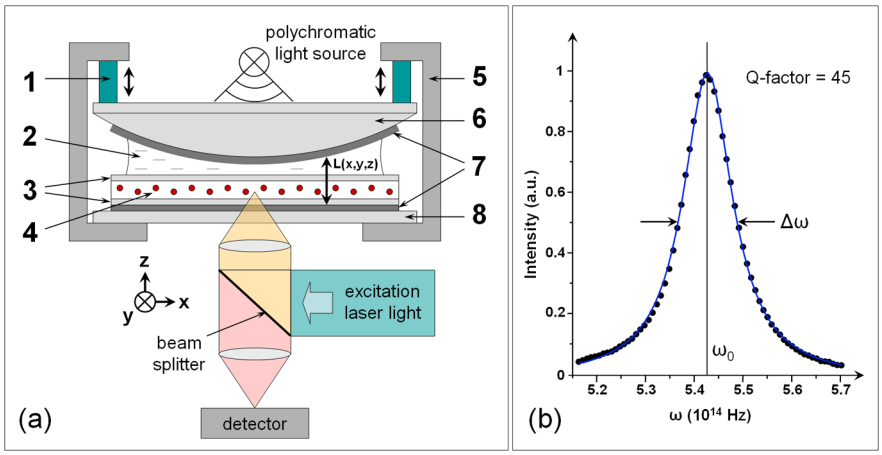

FIG. 1 (color online). (a) Scheme of the experimental setup. The tunable microcavity consists of: 1. Piezoelectric cell, 2. Immersion oil, 3. Silica layers, 4. Polymer (PMMA) layer with PI molecules, 5. Aluminum holder, 6. Lens, 7. Silver layers, 8. Glass coverslide. For more details see main text. (b) Microcavity transmission spectrum fitted by a Lorentzian function (full line) giving a cavity Q-factor = 45.

refractive index $n = 1.46$). The bottom silicon oxide layer serves as a finite spacer between the silver metal and the dye embedding polymer. The upper silicon oxide layer prevents any interaction of embedded dye molecules with atmospheric oxygen during cavity assembly. The top part of the cavity consists of a plane-convex lens ($F = 150$ mm), again covered with a silver layer (94 nm). The intermediate space between the multilayer covered coverslip and the multilayer covered lens was filled with oil (Immersol 518F, Zeiss, refractive index $n = 1.52$). The cavity length could be adjusted with piezo actuators (PSt $150/3.5 \times 3.5/20$, Piezomechanik GmbH) that move the lens toward or away from the bottom coverslip. Silver and oxide layers were made using an evaporation technique reported elsewhere [8]. Absolute thickness values were determined afterward by fitting a transmission spectrum that was recorded using a collimated white light source [see Fig. 1(b)]. Although the resonance peak in the emission spectrum depends on the absolute value of cavity length, the peak width is only determined by the thickness of the various layers (mostly the silver film thickness values). All subsequent fluorescence spectrum measurements were performed close to the center of the lens, where the formed cavity can be considered to be a plane-parallel system.

The dye doped polymer layer was fabricated by spin coating a subnanomolar solution of the perylene derivative *N*-(2,6-diisopropylphenyl)-perylene-3,4-dicarboxymide (abbreviated by PI) in 2% poly(methyl methacrylate) (PMMA) dissolved in dichloromethane. The resulting layer thickness was determined to be around 70 nm by an atomic force microscope (AFM). To obtain a reference spectrum of the PMMA-embedded molecules, a free space sample was prepared by spin coating a thick layer of the same polymer-dye-dichloromethane mixture onto a pure glass coverslip.

All optical measurements were performed using an inverted confocal microscope (based on an Axiovert 135 TV, Zeiss) equipped with a high-numerical-aperture objective [Planeoflex 100/(numerical aperture) = 1.3, Zeiss]. An argon-ion laser (60X-200, American Laser Corporation) at $\lambda = 488$ nm served as excitation source for the fluorescence spectrum measurements. Back-scattered excitation light was blocked with a long-pass filter (Semrock Razor Edge LP02-488RU-25). Fluorescence spectra were acquired with a spectrograph (SpectraPro 300i, Acton Research) in combination with a CCD camera (LNCCD-1340/100-EB/1, Princeton Instruments). For each spectral measurement, the cavity length was adjusted via a defined voltage applied to the piezo actuator. The measurement of each spectrum lasted only three seconds, to prevent premature bleaching, and to reduce the effects of piezo drifting and potential spectral jumps of the molecule (see also below).

Theoretical modeling of the spectrum was done within a semiclassical approach, treating the fluorescing molecule as an oscillating electric dipole emitter and solving Maxwell's equation for the given geometry of the microcavity, see, e.g., Ref. [9] and citations therein. Let us first consider a purely monochromatic emitter. For such an emitter, the electric field amplitude $\vec{E}(\vec{r})$ at position $\vec{r}$ of a free electric dipole emitter within a homogeneous polymer environment is represented by a plane wave expansion (Weyl representation [10]) as

$$\vec{E}(\vec{r}) = \frac{ik^2}{2\pi\epsilon} \int \frac{d\vec{q}}{w} [\vec{\kappa}_p(\vec{\kappa}_p \cdot \vec{p}) + \vec{\kappa}_s(\vec{\kappa}_s \cdot \vec{p})] e^{i\vec{q}\cdot\vec{\rho} + iw|z|}, \tag{1}$$

where $k = \sqrt{q^2 + w^2}$ is the modulus of the wave vector in polymer, $\vec{q}$ and w being its horizontal (two-dimensional vector parallel to cavity interfaces) and vertical (orthogonal to cavity interfaces) components, respectively; ϵ is the dielectric constant of the polymer, which is equal to the square of its refractive index n; and $\vec{p}$ is the amplitude vector of the oscillating dipole. The vector $\vec{\rho}$ is the projection of the position vector $\vec{r}$ onto a plane parallel to the cavity interfaces, and z its projection onto a line orthogonal to these interfaces. Furthermore, it is assumed that the emitter is positioned at coordinates $\vec{r} = (0, 0, 0)$. The unit vectors $\vec{\kappa}_p$ and $\vec{\kappa}_p$ correspond to the p-wave and s-wave contributions (with respect to the cavity interfaces) of the

corresponding plane wave component and are explicitly given by

$$\vec{\kappa}_p = \frac{1}{k}(-w\vec{q}, q), \qquad \vec{\kappa}_s = (\vec{e}_z \times \vec{q}, 0), \tag{2}$$

where $\vec{e}_z$ is the unit vector along the z direction. For modeling the electromagnetic interaction between the emitter and the cavity, one solves Maxwell's equation of the whole cavity system separately for each plane wave component in representation Eq. (1) as source. This is done in a straightforward way by using Fresnel's relations for a planar multilayered system and yields a plane wave representation of the electric field amplitude within each layer of the cavity and in both half-spaces outside the cavity. These representations have the form

$$\vec{E}_j(\vec{r}) = \frac{ik_j^2}{2\pi\epsilon_j}\int \frac{d\vec{q}}{w_j}[\vec{\kappa}_{p,j}(\vec{\kappa}_{p,j}\cdot\vec{p}) + \vec{\kappa}_s(\vec{\kappa}_s\cdot\vec{p})] \cdot e^{i\vec{q}\cdot\vec{\rho}}\cdot[a_j(q)e^{iw_jz} + b_j(q)e^{-iw_jz}], \tag{3}$$

where the ϵ_j, $k_j = \sqrt{q^2 + w_j^2}$, w_j, and $\vec{\kappa}_{p,j}$ correspond now to the jth layer of the system, and the a_j and b_j are the q-dependent coefficients of the plane wave modes traveling toward $+z$ and $-z$, respectively. For the half-space bordering the cavity along the $+z$ direction, there will be no b coefficient, and for the half-space bordering the cavity along the $-z$ direction, there will be no a coefficient (only outgoing waves are admitted).

Knowing the full electric field amplitudes in all layers, two important quantities can be calculated: the total power S_{tot} of emission, and the angular distribution of radiation (ADR) in the half-space toward the light-collecting objective. The total power of emission is found by integrating the positive or negative z component of the Poynting vector $\vec{P} = (c/8\pi)\text{Re}(\vec{E}\times\vec{B}^*)$ over both interfaces of the polymer layer containing the emitting molecule, where the positive sign is chosen for the interface toward the $+z$ direction, and the negative sign for the interface toward the $-z$ direction. The magnetic field amplitude $\vec{B}$ which enters the expression of the Poynting vector is found from Eq. (1) and Eq. (3) using the magnetic induction law from Maxwell's equations. Within the semiclassical interpretation, the total power of emission S_{tot} is proportional to the radiative transition rate of the molecule from its excited to its ground state (at the considered wavelength).

The ADR in the half-space bordering the cavity toward the $-z$ direction (toward the objective) can be found when taking into account that each outgoing plane wave component in the plane wave representation of Eq. (3) is connected with an energy flux proportional to $n_g|b_g|^2$ along the direction $(\vec{q}, -w_g)$, where the subscript g refers now to that half space (glass), and n_g is the corresponding refractive index. Integrating this ADR over the solid angle of light collection of the objective yields a number proportional to the light detection efficiency, C_{det}, of the measurement system for a fluorescent molecule with the given position, orientation, and at the considered wavelength.

The cavity-renormalized spectrum is obtained by calculating $S_{\text{tot}}(\lambda)$ and $C_{\text{det}}(\lambda)$ as functions of the emission wavelength λ. The optical dispersion of the cavity's material, in particular the silver layer, can be taken into account by using the wavelength-dependent refractive index of all materials in the calculations. For the actual cavity considered here, we kept the refractive index values of all dielectrics constant at their values given above, but approximated the wavelength-dependent complex-valued refractive index of silver by a Brendel-Borman model [11]. Knowing both functions $S_{\text{tot}}(\lambda)$ and $C_{\text{det}}(\lambda)$, and the free emission spectrum $F_0(\lambda)$ of the dye in an infinite and pure polymer environment, the emission spectrum $F(\lambda)$ of the dye within the cavity is now obtained (up to a constant factor) by

$$F(\lambda) \propto F_0(\lambda)\frac{C_{\text{det}}(\lambda)S_{\text{tot}}(\lambda)}{\int S_{\text{tot}}(\lambda')d\lambda'}, \tag{4}$$

where $S_{\text{tot}}(\lambda)/\int S_{\text{tot}}(\lambda')d\lambda'$ is proportional to the cavity-induced change of the radiative transition at wavelength λ, and C_{det} is proportional to the probability of detecting a photon at that wavelength.

When fitting experimentally measured spectra, one has two intrinsic unknown fit parameters: the exact position of the molecule within the polymer layer, i.e., its distance from the bottom interface of the polymer layer (interface toward the objective), and its orientation, i.e., inclination toward the z axis. Furthermore, the precise length of the cavity is also not exactly known. Each spectral measurement was done ca. 5 min after adjusting the piezo actuator to a new position. However, there were no means to absolutely measure the cavity length with nanometer resolution, and we observed furthermore a slow (over couple of minutes) drift of the cavity length (due to mechanical relaxation and creeping), which could be seen as a slow shape change of the emission spectrum with time. Thus, the cavity length, i.e., the thickness of the oil layer between the polymer-covering silicon oxide layer and the silver layer on the lens, was used as a third fit parameter. Finally, it was realized that an excellent agreement between calculated and experimentally measured spectra could only be achieved when also taking into account an additional spectral shift of the molecule's emission as commonly observed for single molecule spectra [12].

After selecting a single molecule, we measured several emission spectra for the same molecule at different values of the cavity length. Three prominent spectra are presented in Fig. 2. The figures also show best fits of the calculated spectra to the data. In these fits, the fit parameters, position and orientation of the molecule, were kept constant for all spectra (global fitting). We checked by polarization measurements that there is no reorientation of the molecule and the position of the molecule is fixed. In contrast, cavity length (i.e., oil layer thickness) and spectral shift were allowed to vary from spectrum to spectrum. The calcula-

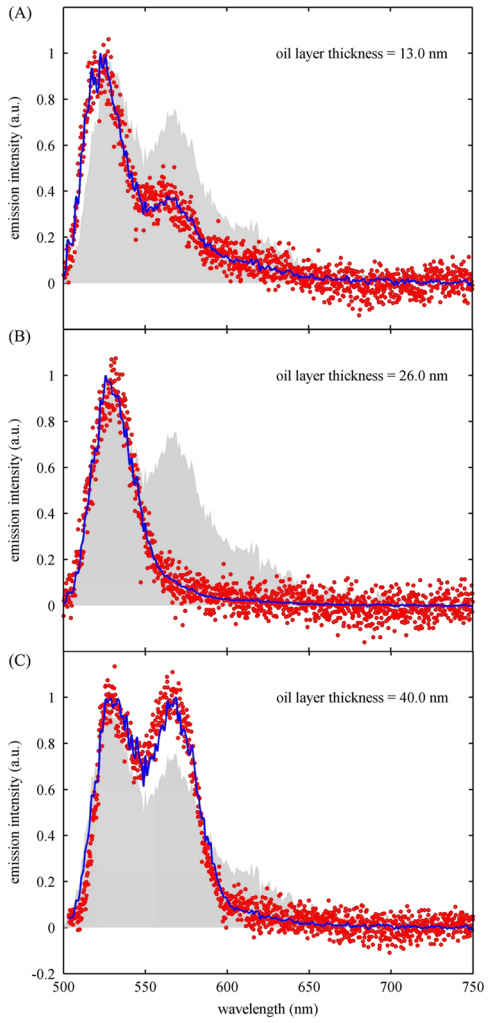

FIG. 2 (color online). Measured spectra (red dots) of a single molecule embedded in the microcavity at various values of cavity length. The blue solid lines show the best fit of a theoretically calculated spectrum, using the free spectrum in polymer (gray shaded area) as the starting point [F_0 in Eq. (4)]. Fitted value of oil layer thickness is indicated in each of the plots. The determined spectral shifts are, from top to bottom, -2 nm, -5 nm, and -14 nm. For better comparison with the free spectrum, the measured and fitted spectra are shown shifted by the opposite of these values toward the red spectral region.

tions showed that the observed molecule was close to the upper polymer interface (toward the oil) and had a nearly vertical orientation. Because of the special electric field configuration of the focused laser light inside the cavity [13], such dipoles are efficiently excited. The obtained values of spectral shift between -2 nm and -14 nm are common when observing single perylene emission spectra, and similar values have been reported before [14]. To quantify fit quality, we calculated the covariance between measured and fitted spectra and found covariance values of better than 0.9. In total, we measured spectra for more than 30 molecules and always found similar excellent agreement between measured and fitted spectra. The reason for the success of the semiclassical model is that we observe molecules that are rather far away from the metal surfaces so that fluorescence quenching is still moderate and nonlocal plasmonic effects (which are not accounted for in our model) do not play a significant role.

In summary the experimental results show that, by tuning the cavity length, one can significantly change the emission spectrum of an individual molecule, and control the ratio of distinct vibronic transition probabilities. The agreement with a theoretical model based on a semiclassical approach is remarkable demonstrating its appropriateness not only for calculating transition rates and ADRs (as was done before) but also for describing cavity-induced changes of the entire emission spectrum.

The authors thank Kirstin Elgass, Sébastien Peter, and Mathias Steiner for fruitful discussions and valuable technical support, and Tyler Arbour for his linguistic advice. Financial support by the European Commission (Marie-Curie Research Training Network NANOMATCH, Contract No. MRTN-CT-2006-035884), the "Kompetenznetz Funktionelle Nanostrukturen Baden-Württemberg" and by the Deutsche Forschungsgesellschaft (project EN 297/12-1) is gratefully acknowledged.

*Present address: Department of Physics, Lund University, SE-22100 Lund, Sweden.
†alfred.meixner@uni-tuebingen.de
‡enderlein@physik3.gwdg.de;
A significant part of the work was done by JE during his stay with Tübingen University.

[1] E. M. Purcell, Phys. Rev. **69**, 681 (1947).
[2] K. Drexhage, Prog. Opt. **XII**, 165 (1974).
[3] R. Chance, A. Prock, and R. Silbey, Adv. Chem. Phys. **37**, 1 (1978).
[4] W. Lukosz, J. Opt. Soc. Am. **69**, 1495 (1979).
[5] M. Lieberherr, C. Fattinger, and W. Lukosz, Surf. Sci. **189–190**, 954 (1987).
[6] F. D. Stefani, K. Vasilev, N. Bocchio, N. Stoyanova, and M. Kreiter, Phys. Rev. Lett. **94**, 023005 (2005).
[7] J. Enderlein, Phys. Chem. Chem. Phys. **4**, 2780 (2002).
[8] M. Steiner, F. Schleifenbaum, C. Stupperich, A. V. Failla, A. Hartschuh, and A. J. Meixner, Chem. Phys. Chem. **6**, 2190 (2005).
[9] J. Enderlein and T. Ruckstuhl, Opt. Express **13**, 8855 (2005).
[10] C. Girard and A. Dereux, Phys. Rev. B **49**, 11 344 (1994).
[11] A. D. Rakić, A. B. Djurišić, J. M. Elazar, and M. L. Majewski, Appl. Opt. **37**, 5271 (1998).
[12] H. P. Lu and X. S. Xie, Nature (London) **385**, 143 (1997).
[13] D. Khoptyar, R. Gutbrod, A. Chizhik, J. Enderlein, F. Schleifenbaum, M. Steiner, and A. J. Meixner, Opt. Express **16**, 9907 (2008).
[14] F. Stracke, C. Blum, S. Becker, K. Müllen, and A. Meixner, Chem. Phys. Chem. **6**, 1242 (2005).